NUCL SCI TECH (2018) 29:81
https://doi.org/10.1007/s41365-018-0414-0

Study on neutronics design of ordered-pebble-bed fluoride-salt-cooled high-temperature experimental reactor

Rui Yan[1] · Shi-He Yu[1] · Yang Zou[1] · Qun Yang[1] · Bo Zhou[1,2] · Pu Yang[1,2] · Hong-Hua Peng[1] · Ya-Fen Liu[1] · Ye Dai[1] · Rui-Ming Ji[1,2] · Xu-Zhong Kang[1] · Xing-Wei Chen[1,2] · Ming-Hai Li[1] · Xiao-Han Yu[1]

Received: 5 September 2017 / Revised: 7 February 2018 / Accepted: 7 February 2018 / Published online: 25 April 2018

Abstract This paper presents a neutronics design of a 10 MW ordered-pebble-bed fluoride-salt-cooled high-temperature experimental reactor. Through delicate layout, a core with ordered arranged pebble bed can be formed, which can keep core stability and meet the space requirements for thermal hydraulics and neutronics measurements. Overall, objectives of the core include inherent safety and sufficient excess reactivity providing 120 effective full power days for experiments. Considering the requirements above, the reactive control system is designed to consist of 16 control rods distributed in the graphite reflector. Combining the large control rods worth about 18000–20000 pcm, molten salt drain supplementary means (− 6980 to − 3651 pcm) and negative temperature coefficient (− 6.32 to − 3.80 pcm/K) feedback of the whole core, the reactor can realize sufficient shutdown margin and safety under steady state. Besides, some main physical properties, such as reactivity control, neutron spectrum and flux, power density distribution, and reactivity coefficient, have been calculated and analyzed in this study. In addition, some special problems in molten salt coolant are also considered, including ^{6}Li depletion and tritium production.

Keywords Ordered-pebble-bed fluoride-salt-cooled high-temperature experimental reactor · Neutronics design · Reactive control · Neutron spectrum · Temperature coefficient

This work was supported by the Chinese Academy of Sciences TMSR Strategic Pioneer Science and Technology Project (No. XDA02010000) & Thorium uranium fuel cycle characteristics and key problem research Project (No. QYZDY-SSW-JSC016).

✉ Yang Zou
zouyang@sinap.ac.cn

[1] Shanghai Institute of Applied Physics, Chinese Academy of Sciences, Shanghai 201800, China

[2] University of Chinese Academy of Sciences, Beijing 100049, China

1 Introduction

The fluoride salt coolant concept originated from the design and construction of a series of molten salt reactors such as aircraft reactor experiment (ARE) [1], molten salt reactor experiment (MSRE) [2, 3], and salt breeder reactor (MSBR) [4, 5] at Oak Ridge National Laboratory (ORNL) from the 1950s to 1970s. Fuel dissolved in molten salt flows in the whole loop system of the reactor. However, due to the complex liquid fuel online processing, structural material irradiation at high temperature, and other political reasons, the technology is difficult to commercialize in a short period of time. At the beginning of this century, the concept of an advanced high-temperature reactor (AHTR) was proposed, for instance, 2400 MW Prism-AHTR (ORNL, SNL, UCB 2001) [6], 2400 MW liquid-salt-cooled very-high-temperature reactor (LS-VHTR) concept design (ORNL, SNL, UCB 2005) [7], pebble bed–AHTR (PB-AHTR) and stringer–AHTR (UW, Areva 2006), 2400 MW integrated pebble bed–AHTR design (UCB 2006) [8], 900 MW modular pebble bed–AHTR (UCB 2008) [9], 3400 and 125 MW plank-type fluoride-salt-cooled reactors (ORNL 2010) [10, 11], and so on. These AHTRs theoretically fit well with the development needs of the Generation IV nuclear power system, including sustainability, economy, safety, reliability, and nuclear non-proliferation. In 2012, IRP was established, and AHTR was officially renamed the fluoride-salt-cooled high-temperature reactors (FHRs) [12]. These four types of FHRs—prismatic, plank, stringer, and pebble bed—have two main characteristics. One is the use of fluoride salt without fuel as coolant, and the other is the use of tristructural isotropic (TRISO) particle fuel elements. Among these options, the pebble fuel has some specific advantages, such as stable structure, radioactivity shielding effect, high mechanical strength, and convenience of transportation and storage, especially in high-temperature gas-cooled reactor applications.

In most existing pebble bed reactors, the fuel pebbles are primarily arranged in order and disordered modes. Susskind [13] and Winsche et al. [14] carried out a large number of experiments into ordered and disordered packing of pebbles. Epel and Levine et al. [15] performed further analysis into the flow resistance of the ordered pebble bed under many different geometric rules in order to determine the best preliminary design for a sodium-cooled fast breeder reactor. In particular, Tian et al. [16, 17] carried out a comprehensive study on ordered pebble beds, including the packing mode, pebble bed geometry, and pebble bed stability features based on a large number of experimental devices and then proposed a new ordered bed modular HTGR reactor concept. However,so far, the ordered pebble bed has not been applied in the FHRs. In this paper, a conceptual 10 MW ordered-pebble-bed fluoride-salt-cooled high-temperature experimental reactor (OPB-FHER) is designed and is aimed at 120 effective full power days with adequate safety when operating in the steady state. Subsequently, some primary design parameters and unique physical properties of this reactor are analyzed, including the reactivity control method, neutron spectrum and flux, power density distribution, reactivity coefficient, ^{6}Li depletion, and tritium production.

2 Core design

2.1 TRISO and fuel pebble

The fuel design is related to the HTR-10 structure with TRISO-coated particles [18], as shown in Fig. 1a. Taking into account the higher volumetric heat capacity of molten salt coolant, as well as the realistic method for obtaining fuel, the uranium loading of a single fuel pebble in this study is increased to 7 g, which relates to the fuel design of HTR-PM [19].

The fuel pebble diameter is 6 cm, including an external graphite shell with a thickness of 0.5 cm and the internal fuel filling zone with a diameter of 5 cm. There are 11669 TRISO particles filled in the fuel filling zone with 7.03% packing fraction. A simple cubic lattice equivalent model is used in this study, as shown in Fig. 1b. Meanwhile, other TRISO particle models, including the equivalently filled regular model, the disturbed regular model, the randomly filled regular model, and the fully random model, have been performed in a series of other studies [20]. The fuel element characteristic parameters are shown in Table 1.

2.2 Fuel pebble arrangement

In the active area, 2-cm-deep grooves are processed in line with surface curvature of the fuel pebbles in the bottom surface of a graphite reflector. These grooves are arranged in a square geography. If pebbles in the first layer fall into the grooves, the center of each series of four pebbles can form a new depression for the second layer, and accumulating layers form a pyramid. In order to keep this stable geometrical condition of the pebble bed, the inner surface of top graphite reflector is also processed with the same method. Besides, the side reflector constitutes an eight edges prism cavity, and the inner surface of the side reflector must be exactly tangent with the surface of the pebbles. In this ordered packed bed, the pebbles can support each other. The structure has strong stability against various changes, such as pressure changes and size or shape changes due to high temperature and strong

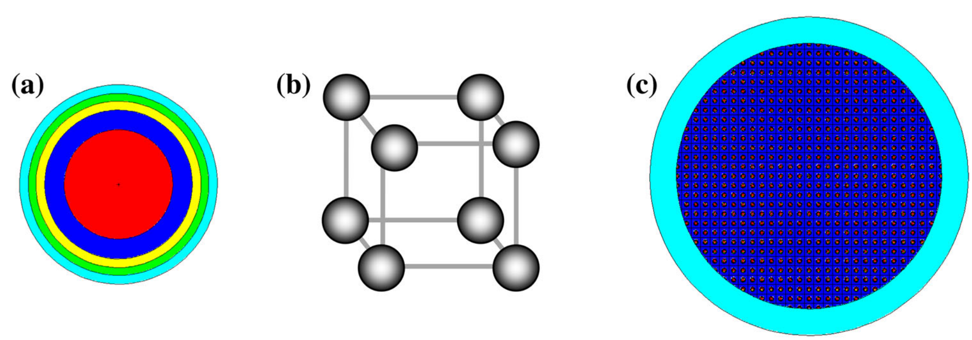

Fig. 1 (Color online) Schematic diagram of TRISO and fuel pebble. **a** TRISO, **b** simple cubic lattice model, **c** fuel pebble model

Table 1 OPB-FHER fuel element characteristic parameters

Parameters	Value
Pebble diameter (cm)	6
Fuel zone diameter (cm)	5
Density of graphite matrix and shell (g cm^{-3})	1.73
^{235}U enrichment (%)	17.08
U loading per pebble (g)	7.0
Kernel diameter (mm)	0.5
UO_2 density (g cm^{-3})	10.4
Layer materials starting from kernel	PrC/PyC/SiC/PyC
Layer thickness (μm)	95/40/35/40
Layer density (g cm^{-3})	1.1/1.90/3.18/1.90

irradiation. Figure 2 shows the arrangement of fuel pebbles. This geometric selection maintains strong structural stability. If the centers of adjacent spheres are separated by 1.167 times their diameter (7.0 cm), the core can still maintain a relatively regular arrangement with sufficient constant packing fraction (PF) when the active surface area changes by less than 5% [17]. Under such condition, the vertical distance between the centers of two adjacent spheres is 0.5652 times the diameter of the ball (3.3912 cm), and the corresponding theoretical packing fraction is 68%.

2.3 Core layout and fuel loading

The core model is demonstrated in Fig. 3. From the inside out, the core of the OPB-FHER mainly consists of the activity area, a graphite reflector, and the core barrel. The active area is approximately an octagonal prism with 185.0 cm height and two groups of edge distance of 111.0 and 114.9 cm, respectively, which forms a boundary that keeps the forces regular accumulation as mentioned above. The core is filled with 11043 fuel pebbles and 432 graphite pebbles. The reflector periphery size is 300 cm in height and 260 cm in diameter. With a 2-cm-thick metal barrel, the overall core size is 304 cm in height and 264 cm in diameter.

The packing fraction (PF) of pebbles in the active area due to accumulation can reach 68 and 65.8% for theoretical mode and the actual value, respectively. This fine distinction of PF is produced in the boundary effect. In this packing, some stable natural channels for the flow of molten salt can be formed among the pebbles from the bottom up. Graphite pebbles with 6.0 cm diameter at the top and bottom can form a transition zone between the fuel pebbles and graphite reflector, which can prevent overheating damage for fuel pebbles at the top and bottom due to a lack of coolant. There are 20 channels distributed in the graphite reflector, including 16 for control rods and 4 for experiments. A total of 201 coolant flow channels each with 4 cm diameter are arranged in the top and bottom reflector.

For fuel management, whole loading and unloading are adopted in one cycle. Each cycle has one batch of fuel consisting of 11043 fuel pebbles and 432 graphite pebbles. The basic physical parameters for the core of one cycle are listed in Table 2.

2.4 SCALE codes and data

The SCALE code system [21] developed at Oak Ridge National Laboratory has been used for many years for various light water reactor applications. In recent years, features have been added that allow handling of problems specific to high-temperature gas-cooled reactors. Such specific features include the treatment of the double heterogeneity of fuel that is characteristic of HTGRs, for both the prismatic and pebble bed designs. Furthermore, it does account for the double heterogeneity of the fuel through the way the cross section self-shielding is carried out by using the DOUBLEHET cell data option for cross section processing [22]. All neutronics physics calculations and simulations described in this paper were performed with KENOVI in SCALE6.1 and used nuclear cross

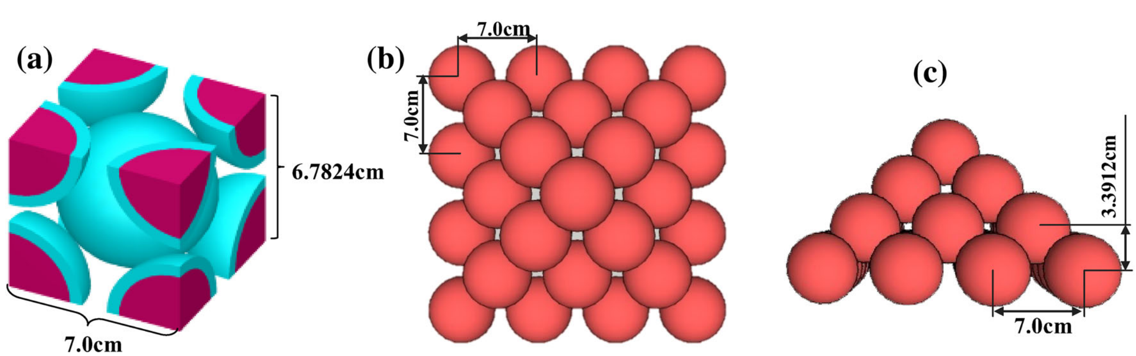

Fig. 2 (Color online) Ordered packing schematic diagram. **a** Pebble packing model, **b** horizontal direction array, **c** vertical direction array

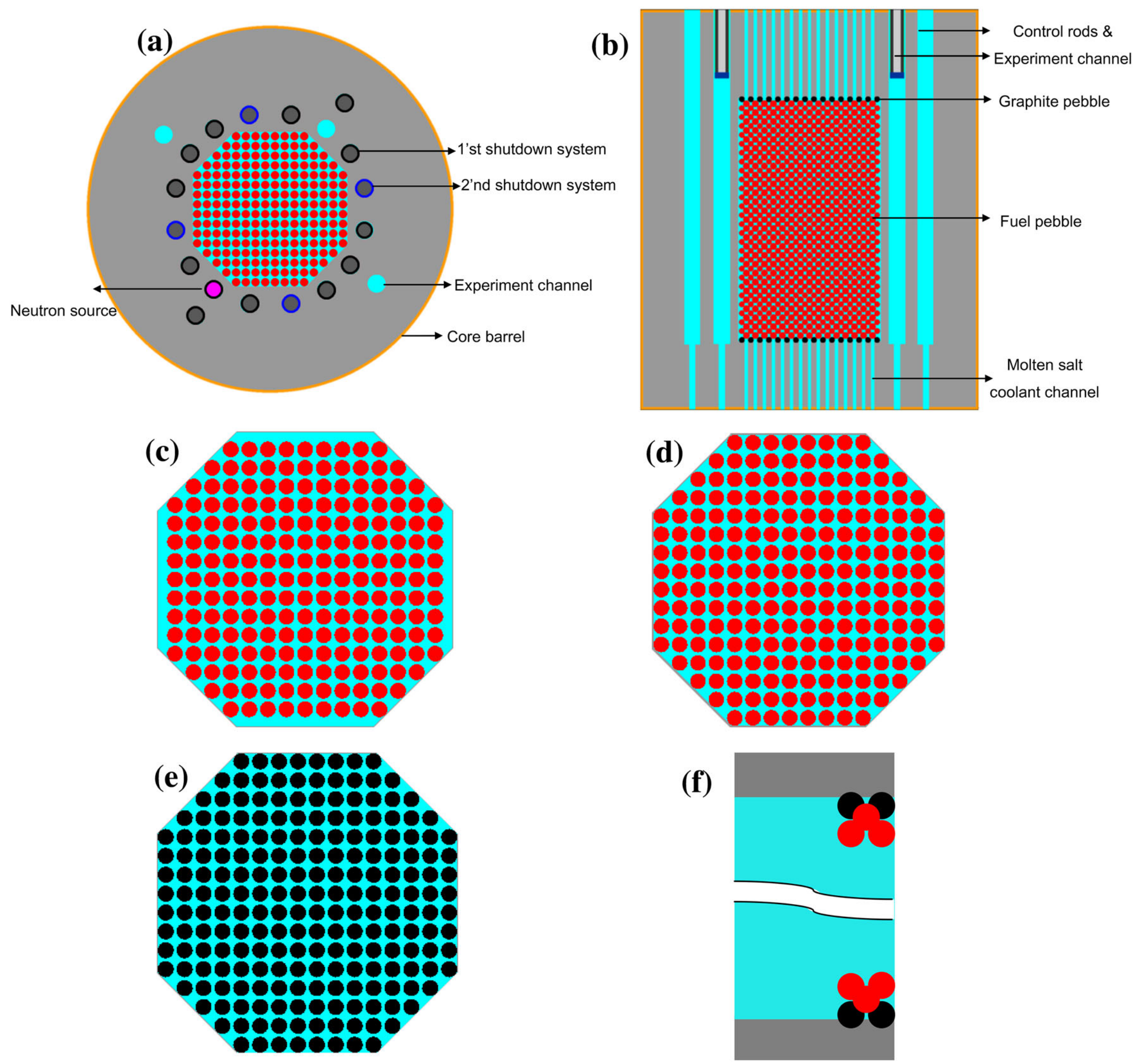

Fig. 3 (Color online) Core of the OPB-FHER. **a** Core cross section, **b** core longitudinal section, **c** fuel pebble array-layer I, **d** fuel pebble array-layer II, **e** graphite pebble array, and **f** top and bottom structure

sections based on ENDF/B-VII.0 data that were further processed by the CSAS6 sequence of SCALE in energy libraries for 238 groups. The TRITON control module, couple KENOVI, and ORIGENS were used for burnup analysis in SCALE.

3 Core physical properties

3.1 Reactivity control

Two independent reactivity control systems with two radial positions are set in the graphite reflector, as shown in Fig. 2a. The first system consists of 10 rods in the inner circle and 2 rods in the outer circle surrounding the active area. These rods provide power regulation, burnup compensation, temperature control, and shut down at all kinds of operating conditions. The second reactivity control system is composed of 4 rods in the inner circle (marked in blue) that force shutdown when the first shutdown system fails to perform properly. The absorber material is B_4C (19.9 at.% ^{10}B) under Hastelloy-N alloy cladding. The inner and outer diameters of the control rod are 55 and 110 mm, respectively. The specific structural parameters and material composition of the control rod are shown in Fig. 4 and Table 3.

Three main temperature states are analyzed in the core design, namely, 615, 590, and 459 °C, representing the power operation status, normal cold status, and accident cold status, respectively. Table 4 shows the reactivity compensation and reactor safety requirements. It can be seen that the first shutdown system can provide 15120–15820 pcm worth with 12 rods at different lifetime stages. Thus, it has sufficient margin at various working

Table 2 Main parameters of the core

Parameters	Value
Power	10 MW_{th}
Effective full power days	> 120 day
Fuel type	UO_2 (17.08 wt.% U-235 enrichment)
Fuel loading per cycle	13.2 kg
Fuel element type	UO_2 fuel pebble
Fuel element quality	11043
Fuel elements array	Ordered packing
Active area volume	1.95 m^3
Core diameter	264 cm
Core height	304 cm
The primary loop coolant	2LiF-BeF_2(99.99 at.% ^{7}Li)
Inlet/outlet temperature@10 MW_{th}	600/628 °C
Mass flow rate of coolant@10 MW_{th}	150 kg/s
shutdown depth	− 2000 pcm
Average burnup depth @120EFPD	14.6(GWd/MTU)
Maximum pressure	< 0.5 MPa

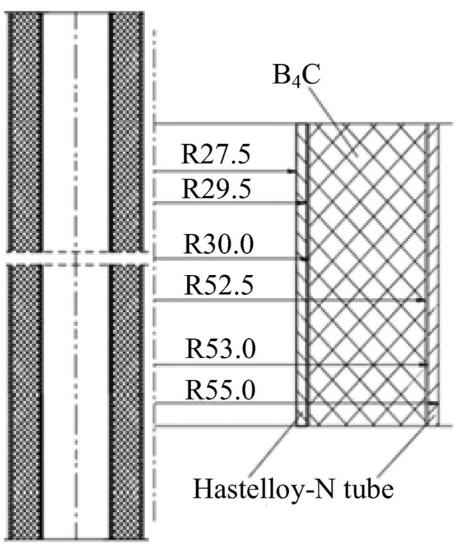

Fig. 4 Control rod geometry

conditions, including the extreme accident state, the FLiBe's melting point 459 °C, and single-rod failure accident (seen as the − 8310 to − 4620 pcm shutdown depth of 11 rods). The second shutdown system also has sufficient margin of about − 4320 to − 3420 pcm, even at 590 °C. All the control rods are worth about 18000–20000 pcm. If the accident is out of control for the second system of rods, the molten salt drain system will be in the working condition, which can provide a maximum of − 6980 pcm reactivity and guarantee safe reactor shutdown.

3.2 Neutron spectrum

The neutron spectrum is dependent on fuel composition, moderator type, and the structural materials of reactor core, and it determines the basic physical properties of the core. Therefore, it is important to analyze the neutron spectrum in the reactor design. Figure 5 shows the normalized neutron spectrum for different single fuel cells in 3 typical reactors. The HTR and OPB-FHER used the same lattice model geometry shown in Fig. 2a. The difference between the two models is the use of different coolants.

Table 3 Materials of control rod

Radial radius (mm)	Materials	Density (g/cc)
0–27.5	Void	0
27.5–29.5	Hastelloy-N (Ni-Mo-Cr–Fe–Mn–Si-Al Bal-16.50–7.03–4.24–0.50–0.32–0.19)	8.86
29.5–30	Void	0
30–52.5	B_4C (19.9 at.% ^{10}B)	2.1
52.5–53	void	0
53–55	Hastelloy-N (Ni–Mo–Cr–Fe–Mn–Si–Al	8.86

Table 4 Reactivity compensation

Core status	Beginning life	Mid-life	End of life
Excess reactivity (pcm[a])			
Normal cold 590 °C	6810 (39*)	4890 (39)	3770 (39)
Accident cold 459 °C	8860 (38)	6780 (38)	5800 (40)
Shutdown margin @Normal cold 590 °C (pcm[a])			
12 rods of first shutdown system	− 8310 (40)	− 10700 (38)	− 12050 (38)
11 rods of first shutdown system	− 4620 (38)	− 7040 (38)	− 8310 (39)
4 rods of second shutdown system	− 3420 (37)	− 3850 (38)	− 4320 (38)
Supplementary shutdown means			
Molten salt drain reactivity (pcm*)	− 6980 (37)	− 4574 (38)	− 3651 (40)

[a]Reactivity calculated with KENOVI in SCALE6.1

*Average statistical error

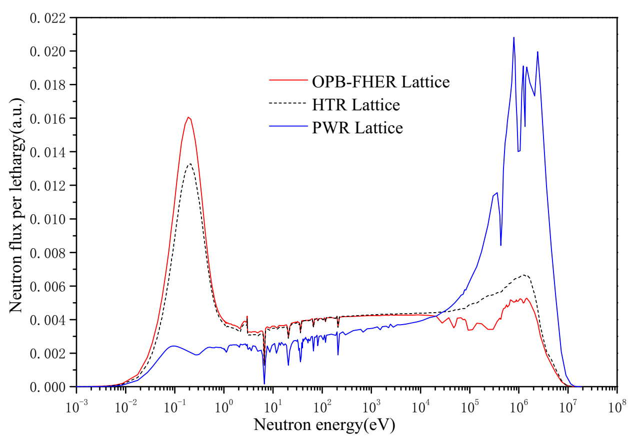

Fig. 5 (Color online) Neutron spectrum for different reactor elements

The square unit cell model of a standard Westinghouse 17 × 17-lattice assembly is adopted as a reference for pressurized water reactor (PWR). In the PWR pin cell model, the value of the fuel pellet radius, fuel pellet to cladding gap, cladding inner radius, cladding outer radius, and pin pitch were 0.4096, 0.0082, 0.4178, 0.4750, 1.26 cm, respectively. In addition, the three cell models used the same level of ^{235}U enrichment (17.08%) but different coolant, followed by helium, molten salt, and water. Further, the white reflection boundary condition is used in the calculation with SCALE.

It can be seen that, no matter what core material is used, the neutron energy spectrum has two peaks consisting of the fission energy spectrum in the fast area and the Maxwell spectrum in the thermal area. As high-enrichment fuel was used in the calculation, the energy spectrum of this PWR occupies the high-energy region compared to that in PWR, and the peak in thermal area is not obvious. The shape of the neutron energy spectrum is different in a high-temperature gas-cooled reactor. It has a higher peak in thermal area and a lower peak in fast area, in contrast to the spectrum in PWR. This distinction arises because the proportion of coated particle fuel is much lower than in PWR. Thus, the macro-absorption cross section of the thermal neutron in the core region of the OPB-FHER is much smaller than that in PWR, resulting in a high proportion of thermal neutrons. The neutron spectrum in a molten salt pebble-bed reactor is similar to that in a high-temperature gas-cooled reactor for the same fuel pebble. But due to the moderation and neutron absorption effect in BeF_2-2LiF, the OPB-FHER spectrum occupies a slightly lower energy region.

3.3 Neutron flux density and power density distribution

In this section, four control rods were inserted into the core in order to reach criticality during analysis. The neutron flux density distributions in the core active area at the beginning of life with xenon equilibrium are shown in Fig. 6. The coordinate origin is the center of the active region. The total flux density is about 0.5–1.45 × 10^{14} n/cm^2/s. The maximum radial neutron flux density is in the center of the active area. However, the maximum axial neutron flux density appears at about 20 cm below the center plane, and this downward shift of the maximum flux density is due to the insertion of the control rods.

For the calculation of power density distribution (Fig. 7), the active area is divided into 27 meshes with 6.7824 cm size in the axial direction. The maximum axial power density is 11.40 W/cm^3, located 20 cm below the center of the active area. The axial average power density is 9.10 W/cm^3. The axial power peak factor is 1.25.

The radial mesh size is 7 cm × 7 cm. The radial maximum and mean power density are 9.10 and 7.56 W/cm^3, respectively. The radial power factor is 1.20. Therefore, the total power peak factor is 1.25 × 1.20 = 1.50 for the core active area.

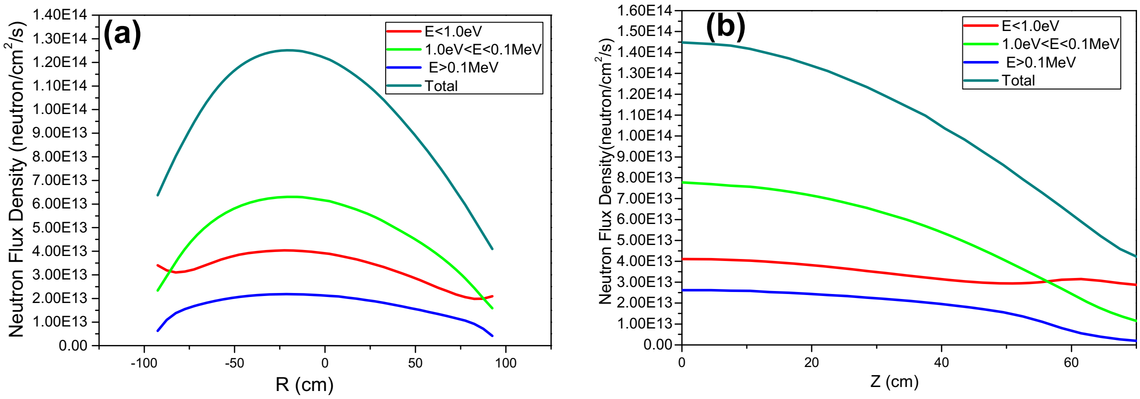

Fig. 6 (Color online) Neutron flux density in the active area at beginning of life with xenon equilibrium. **a** Axial neutron flux density, **b** radial neutron flux density

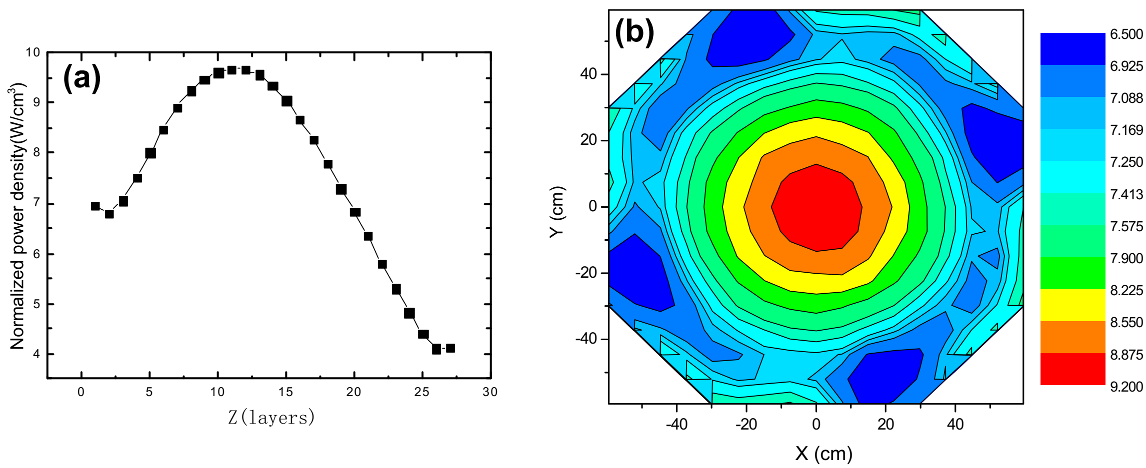

Fig. 7 (Color online) Power density distribution in the active area at beginning of life with xenon equilibrium. **a** Axial power density distribution, **b** radial power density distribution (W/cm^3)

Using a thermal hydraulic calculation, the maximum average temperature of the fuel pebble in the core is found to be 682 °C and appears 20 cm below the center.

3.4 Temperature coefficients of reactivity

Reactivity temperature coefficients are the key parameters for assessing reactor safety, which primarily includes the contribution of fuel, coolant, moderator, and reflector. In this study, the KENO module in SCALE6.1 code is used to calculate K_{eff} for these coefficients. Statistical uncertainty is inherent in the Monte Carlo method, and K_{eff} was calculated at multiple temperature points. The 1/K quadratic curve fitting method or linear fitting [22] was used to process the data. All results at different burning lifetime for one cycle are shown in Table 5.

The fuel reactivity temperature coefficient exists due to the Doppler effect. In the OPB-FHER, the fuel reactivity temperature coefficient is − 2.71 to − 2.35 pcm/K, which agrees well with LWR. The coolant reactivity temperature coefficient, also called the void coefficient, is slightly negative due to thermal expansion of the coolant. The moderator reactivity temperature coefficient is − 3.98 to − 3.11 pcm/K. The total reactivity temperature coefficient is negative throughout the reactor lifetime, illustrating the safety of the reactor to some extent.

Table 5 Temperature coefficients of reactivity

Core status			
TC (pcm/K)	Beginning life	Mid-life	End of life
Fuel	− 2.71	− 2.56	− 2.35
Coolant	− 1.50	− 0.40	− 0.66
Moderator	− 3.98	− 3.11	− 3.39
Reflector	2.54	1.78	1.90
Total	− 6.32	− 4.20	− 3.80

3.5 Burnup, ^{6}Li depletion, and tritium production

The burnup time of one cycle for the core is analyzed as shown in Fig. 8. If $K_{eff} = 1$ was selected as the lifetime truncation, equivalent full power operation will exceed 120 days.

In addition to the initial ^{6}Li stock in the FLiBe coolant, ^{6}Li is a strong neutron absorber in molten salt and is primarily produced through the ^{9}Be (n, nt)→^{6}Li nuclear reaction and removed through the ^{6}Li (n, t)→^{4}He reaction [23]. The consumption and production rates for ^{6}Li in molten salt are related to the core power, and they eventually reach a balance after a very long runtime [9]. Figure 9 shows the concentration change of ^{6}Li along with the burnup time. It is seen that the concentration of ^{6}Li declines gradually in a short-to-medium term, just like burnable poison. However, if the reactor was operated in a very long time, the ^{6}Li quantity will reach a steady state. Therefore, the reactivity will be released at last, which needs to be considered and analyzed for long runtimes.

Tritium is a very lively nuclide that is easy to spread and causes a hydrogen embrittlement effect in structural materials. In addition, it has strong radioactivity both in the working environment of the nuclear power plant and the natural environment outside the plant [24]. Therefore, tritium production is an important source term and should be considered in the design of radiation protection, including its behavior in the reaction channel and its accumulation, dissolution, and diffusion in the reactor components. In a 10 MW OPB–FHER reactor, ^{6}Li in FLiBe coolant is the main production source of tritium by the nuclear reaction $^6\text{Li} + \text{n} \rightarrow {}^3\text{H} + {}^4\text{He} + 4.79$ MeV [25]. Moreover, some ^{7}Li can also generate tritium through the nuclear reaction $^7\text{Li} + \text{n} \rightarrow {}^3\text{H} + {}^4\text{He} + \text{n}$. Figure 9 shows the tritium concentration in the 10 MW OPB-FHER over short-to-medium timescales.

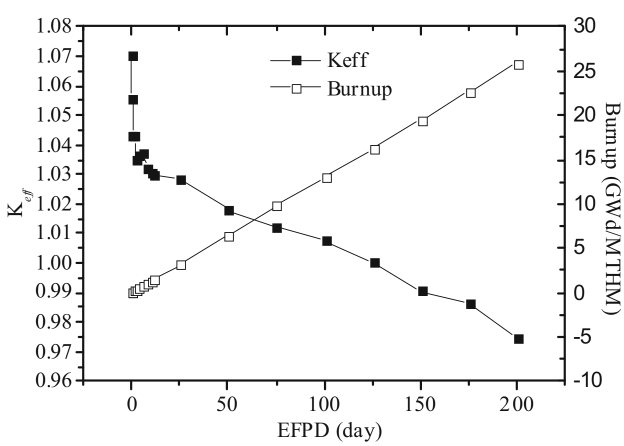

Fig. 8 K_{eff} change over equivalent full power running time

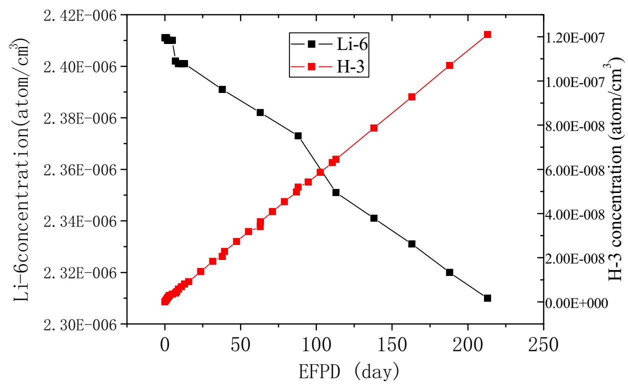

Fig. 9 Concentration variation of ^{6}Li and ^{3}H

4 Conclusion

A conceptual design of a 10 MW OPB-FHER in presented in this study. The neutronic physics parameters are calculated and analyzed. The following primary conclusions can be drawn:

(1) A stable and compact pebble core can be delicately constructed that achieves the design goals of 100 EFPD.
(2) By combining large control rods worth about 18000–20000 pcm, molten salt drain supplementary means (− 6980 to − 3651 pcm), and negative temperature coefficient (− 6.32 to − 3.80 pcm/K) feedback within the core, the reactor can have a sufficient shutdown margin and operate safely in the steady state.
(3) The shape of the neutron spectrum is similar to that in a high-temperature gas-cooled reactor, but is softer in the thermal range due to the moderation of molten salt coolant.
(4) As lithium fluoride and beryllium fluoride molten salts are used in the reactor, tritium production by ^{6}Li reactions should be considered during radioactive safety assessment.

Owing to the application of graphite materials, differential thermal expansion will cause certain stresses in the ordered bed and engineering the restraint system will be a challenge. In the next step, theoretical simulation of the thermal expansion of the fuel pebble based will be carried out to study its effect on the reactor physics. A steady-state analysis for one cycle was performed in this study. Circulating charging may improve the fuel economy, but a positive temperature coefficient of the reflector might be an unstable factor. Therefore, accident scenarios analysis and fuel management optimization must be examined in the future.

References

1. E.S. Bettis, W.B. Cottrell, E.R. Mann et al., The aircraft reactor experiment—operation. Nucl. Sci. Eng. **2**, 841–853 (1957)
2. A.M. Weinberg, M.W. Rosenthal, P.N. Haubenreich et al., Collection of papers on the molten salt reactor experiment. Nucl. Appl. Technol. **8**(2), 105–219 (1970)
3. D. Scott, A.G. Grindell, *Components and Systems Development for Molten Salt Breeder Reactors*. (Oak Ridge National Laboratory, Oak Ridge, Tennessee, 1967), ORNL Report-TM-1855. https://doi.org/10.2172/4367859
4. R.C. Robertson, O.L. Smith, R.B. Briggs et al., *Two-fluid Molten-Salt Breeder Reactor Design Study*. (Oak Ridge National Laboratory, Oak Ridge, Tennessee, 1970), ORNL Report-4528. https://doi.org/10.2172/4093364
5. J.L. Anderson, P.N. Haubenreich, R.C. Robertson et al. *Conceptual Design Study of a Single-fluid Molten Salt Breeder Reactor*. (Oak Ridge National Laboratory, Oak Ridge, Tennessee, 1971), ORNL Report-4541. https://doi.org/10.2172/4030941
6. C.W. Forsberg, The advanced high-temperature reactor: high-temperature fuel, liquid salt coolant, liquid-metal-reactor plant. Prog. Nucl. Energy **47**, 32–43 (2005)
7. D.T. Ingersoll, *Status of Physics and Safety Analyses for the Liquid-Salt-Cooled Very High-Temperature Reactor (LS-VHTR)*. (Oak Ridge National Laboratory, Oak Ridge, Tennessee, 2005), Technical Report ORNL/TM-2005/218. https://doi.org/10.2172/885991
8. C.W. Forsberg, P. F. Peterson, R.A. Kochendarfer, in *Design Options for the Advanced High-Temperature Reactor*. Paper 8026 Proceedings of ICAPP'08, (Anaheim, California, June 8–12, 2008)
9. R. Hong, S. Huber, K. Lee et al., *Reactor Safety and Mechanical Design for the Annular Pebble-bed Advanced High Temperature Reactor 2009 NE 170 Senior Design Project*. Report UCBTH09-001, (University of California, Berkeley, May 19 2009)
10. D. Ilas, D.E. Holcomb, V.K. Varma, *Advanced High-Temperature Reactor Neutronic Core Design*, Proceedings of PHYSOR 2012—Advances in Reactor Physics—Linking Research, Industry, and Education Knoxville, Tennessee, USA, on CD-ROM, American Nuclear Society, (Oak Ridge National Laboratory, LaGrange Park, IL, April 15–20, 2012)
11. S.R. Greene, J.C. Gehin, D.E. Holcomb et al., *Pre-Conceptual Design of a Fluoride-Salt-Cooled Small Modular Advanced High Temperature Reactor (Sm AHTR)*. Technical Report TM-2010/199, (Oak Ridge National Laboratory, Tennessee, 2011). https://doi.org/10.2172/1008830
12. Preliminary Fluoride Salt-cooled High Temperature Reactor (FHR) Subsystem Definition, Functional Requirement Definition and Licensing Basis Event (LBE) Identification White Paper. UCBTH-12-001, IRP Workshop1 UCB. (2012)
13. H. Susskind, W.E. Winsche, W. Becker, Ordered packed-bed fuel elements. Nucl. Technol. **1**, 405–411 (1965)
14. H. Susskind, W. Becker, Pressure drop in geometrically ordered packed beds of spheres. AIChE J. **13**, 1155–1159 (1967)
15. L.G. Epel, M.M. Levine, G. Nugent, R.J. Parsick, The ordered-bed fast react or concept − 1000 MW e reactor design. Technical Report BNL 50027 (T-444), (1966). https://doi.org/10.2172/4569130
16. J.F. Tian, A new ordered bed modular reactor concept. Ann. Nucl. Energy **34**, 297–306 (2007). https://doi.org/10.1016/j.anucene.2007.01.003
17. J.F. Tian, Advanced ordered bed modular HTGR reactor concept. Chin. J. Nucl. Sci. Eng. **38**, 147–157 (2008)
18. X.Q. Jing, Y.W. Yang, Y.X. Gu et al., Prediction calculation of HTR-10 fuel loading for the first criticality. J. Tsinghua Univ. Sci. Technol. **41**, 116–119 (2001). **(in Chinese)**
19. Z.Y. Zhang, Z.X. Wu, Y.H. Xu et al., Design of Chinese modular high-temperature gas-cooled reactor HTR-PM. in *Proceedings of 2nd International Topical Meeting on High Temperature Reactor Technology*. (Beijing, September 22–24, 2004)
20. R.M. Ji, R. Yan, X.X. Li et al., Effect of TRISO-particles distributions in pebble fuel. Nucl. Tech. **40**, 100604 (2017). https://doi.org/10.11889/j.0253-3219.2017.hjs.40.100604. **(in Chinese)**
21. W.J. Marshall, B.T. Rearden, *Criticality Safety Validation of Scale 6.1*. (Radiations Safety Information Computational Center, Oak Ridge National Laboratory, Oak Ridge, Tennessee, 2011), Technical Report ORNL/TM-2011/450. https://doi.org/10.2172/1028760
22. Dan Ilas, Scale code validation for prismatic high-temperature gas-cooled reactors. Am. Nucl. Soci. Nucl. Technol. **183**, 379–390 (2013)
23. R.M. Ji, M.H. Li, Y. Zou et al., Impact of photoneutrons on reactivity measurements for TMSR-SF1. Nucl. Sci. Tech. **28**, 76 (2017). https://doi.org/10.1007/s41365-017-0234-7
24. Y. Huang, W. Liu, D.T. Xiao et al., Control and monitoring of tritium in molten salt reactor. Nucl. Tech. **34**, 632–636 (2011). **(in Chinese)**
25. C. Peng, X.W. Zhu, G.Q. Zhang et al., Issues in the calculation of the tritium production of the fluoride-salt-cooled high-temperature reactors using SCALE. Nucl. Tech. **38**, 080601 (2015). https://doi.org/10.11889/j.0253-3219.2015.hjs.38.080601. **(in Chinese)**